Romanian Reports in Physics, Vol. 63, No. 3, P. 624–640, 2011

FROM GIANT OCEAN SOLITONS TO CELLULAR IONIC NANO-SOLITONS

MILJKO V. SATARIĆ[1], MILE S. DRAGIĆ[2], DALIBOR L. SEKULIĆ[1]

[1]Faculty of Technical Sciences, University of Novi Sad, Trg Dositeja Obradovića 6, 21000 Novi Sad, Serbia, E-mail: bomisat@neobee.net, Email: dalsek@yahoo.com
[2]Production "Mile Dragić", Makedonska 2, 23000 Zrenjanin, Serbia,
E-mail: mdragic@armyequipment.com

Received January 14, 2011

Abstract. It is well known that soliton bearing nonlinear differential equations show up in many areas of physics when waves can propagate in a weakly nonlinear and dispersive media. Here we will show the surprising analogy between the single hump solitary waves appearing in long wave regimes in relatively shallow water and mathematically quite similar description of nano-solitons of ionic waves propagating along microtubules in living cells.

Key words: soliton, Laplace and Euler equations, microtubule, nonlinear transmission line, ionic waves.

1. WEAKLY NONLINEAR SHALLOW WATER WAVE REGIME

We first consider an inviscid, incompressible and non-rotating flow of fluid of constant depth h. We take the direction of flow as x-axis and z-axis positively upward the free surface in gravitational field. The free surface elevation above the undisturbed depth h is $\eta(x, t)$, so that the wave surface at height $z = h + \eta(x, t)$, while $z = 0$ is horizontal rigid bottom [1, 2, 3].

Let $\varphi(x, z, t)$ be the scalar velocity potential of the fluid lying between the bottom ($z = 0$) and free space $\eta(x, t)$, Fig. 1. Then we could write the Laplace and Euler equation with the boundary conditions at the surface and at the bottom, respectively, as follows:

$$\frac{\partial^2\varphi}{\partial x^2} + \frac{\partial^2\varphi}{\partial z^2} = 0 \ ; \qquad 0 < z < h + \eta \ ; \qquad -\infty < x < +\infty \tag{1}$$

$$\frac{\partial\varphi}{\partial t} + \frac{1}{2}\left(\frac{\partial\varphi}{\partial x}\vec{i} + \frac{\partial\varphi}{\partial z}\vec{k}\right)^2 + g\eta = 0 \ ; \qquad z = h + \eta \tag{2}$$

$$\frac{\partial \eta}{\partial t} + \frac{\partial \eta}{\partial x}\frac{\partial \varphi}{\partial x} - \frac{\partial \varphi}{\partial z} = 0 \qquad (3)$$

$$\frac{\partial \varphi}{\partial z} = 0 \ ; \qquad z = 0 \ . \qquad (4)$$

It is useful to introduce two following fundamental dimensionless parameters:

$$\sigma = \frac{\eta_0}{h} < 1 \ ; \qquad \delta = \left(\frac{h}{l}\right)^2 < 1 \ , \qquad (5)$$

where η_0 is the wave amplitude (Fig. 1), and l is the characteristic length-like wavelength. Accordingly, we also take a complete set of new suitable non-dimensional variables:

$$X = \frac{x}{l} \ ; \quad Z = \frac{z}{h} \ ; \quad \tau = \frac{ct}{l} \ ; \quad \Psi = \frac{\eta}{\eta_0} \ ; \quad \Phi = \frac{h}{\eta_0 lc}\varphi \ , \qquad (6)$$

where $c = \sqrt{gh}$ is the shallow-water wave speed, with g being gravitational acceleration.

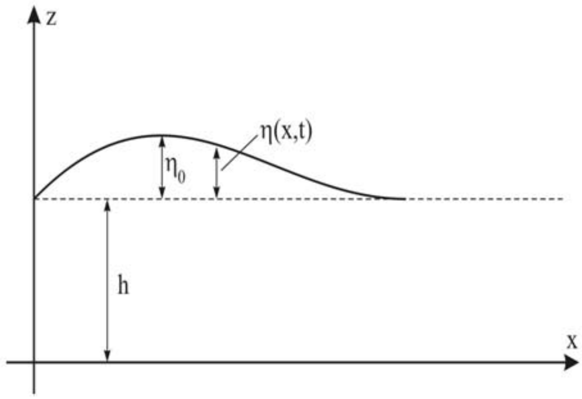

Fig. 1 – The shape of gravitational water wave for fixed t with characteristic parameters: h is undisturbed depth and η is the wave elevation with η_0 being its amplitude.

In terms of (5) and (6) the initial system of equations (1), (2), (3) and (4) now reads

$$\delta\frac{\partial^2 \Phi}{\partial X^2} + \frac{\partial^2 \Phi}{\partial Z^2} = 0 \ ; \qquad (7)$$

$$\frac{\partial\Phi}{\partial\tau}+\frac{\sigma}{2}\left(\frac{\partial\Phi}{\partial X}\right)^2+\frac{\sigma}{2\delta}\left(\frac{\partial\Phi}{\partial Z}\right)^2+\Psi=0\ ;\qquad Z=1+\sigma\Psi\ , \tag{8}$$

$$\frac{\partial\Psi}{\partial\tau}+\sigma\left(\frac{\partial\Phi}{\partial X}\frac{\partial\Psi}{\partial X}\right)-\frac{1}{\delta}\frac{\partial\Phi}{\partial Z}=0\ ;\qquad Z=1+\sigma\Psi\ , \tag{9}$$

$$\frac{\partial\Phi}{\partial Z}=0\ ;\qquad Z=0\ . \tag{10}$$

Expanding $\Phi(x, \tau)$ in terms of δ

$$\Phi=\Phi_0+\delta\ \Phi_1+\delta^2\Phi_2\ , \tag{11}$$

and using the dimensionless wave particles velocity in x-direction, by the definition $u = \partial\Phi/\partial X$, then substituting of (11) into (7-9), with retaining terms up to linear order of small parameters (δ, σ) in (8), and of second order in (9), we get

$$\frac{\partial\Phi_0}{\partial\tau}-\frac{\delta}{2}\frac{\partial^2 u}{\partial\tau\partial X}+\Psi+\frac{1}{2}\sigma u^2=0\ , \tag{12}$$

$$\frac{\partial\Psi}{\partial\tau}+\sigma u\frac{\partial\Psi}{\partial X}+\frac{1}{\delta}\left(1+\sigma\Psi\right)\frac{\partial u}{\partial X}=\frac{\delta}{6}\frac{\partial^3 u}{\partial X^3}\ . \tag{13}$$

Making the differentiation of (12) with respect to X, and rearranging (13), we get

$$\frac{\partial u}{\partial\tau}+\sigma u\frac{\partial u}{\partial X}+\frac{\partial\Psi}{\partial X}-\frac{1}{2}\delta\frac{\partial^3 u}{\partial X^2\partial\tau}=0\ , \tag{14}$$

$$\frac{\partial\Psi}{\partial\tau}+\frac{\partial}{\partial X}\left[u\left(1+\sigma\Psi\right)\right]-\frac{1}{6}\delta\frac{\partial^3 u}{\partial X^3}=0\ . \tag{15}$$

Returning back to dimensional variables $\eta(x, t)$ and $\mathrm{v} = \mathrm{d}\varphi/\mathrm{d}x$, (14) now reads

$$\frac{\partial \mathrm{v}}{\partial t}+\mathrm{v}\frac{\partial \mathrm{v}}{\partial x}+g\frac{\partial\eta}{\partial x}=\frac{1}{3}h^2\frac{\partial^3 \mathrm{v}}{\partial x^2\partial t}\ . \tag{16}$$

We could define the new function $\mathrm{V}(x, t)$ unifying the velocity and displacement of water particles as follows:

$$\mathrm{v}=\frac{1}{h}\frac{\partial \mathrm{V}}{\partial t}\ ;\qquad \eta=-\frac{\partial \mathrm{V}}{\partial x}\ , \tag{17}$$

implying that (16) becomes

$$\frac{\partial^2 \mathrm{V}}{\partial t^2}-gh\frac{\partial^2 \mathrm{V}}{\partial x^2}+\frac{1}{2h}\frac{\partial}{\partial x}\left(\frac{\partial \mathrm{V}}{\partial t}\right)^2=\frac{1}{3}h^2\frac{\partial^4 \mathrm{V}}{\partial x^2\partial t^2}\ . \tag{18}$$

We seek for traveling wave solutions with moving coordinate of the form $\xi = x - \mathrm{v}t$ and with wave speed v, which reduces (18) into ordinary nonlinear differential equation as follows:

$$\left(\mathrm{v}^2 - gh\right)\frac{\mathrm{d}^2\mathrm{V}}{\mathrm{d}\xi^2} + \frac{\mathrm{v}^2}{2h}\frac{\mathrm{d}}{\mathrm{d}\xi}\left(\frac{\mathrm{dV}}{\mathrm{d}\xi}\right)^2 - \frac{\mathrm{v}^2 h^2}{3}\frac{\mathrm{d}^4\mathrm{V}}{\mathrm{d}\xi^4} = 0 . \tag{19}$$

Integrating (19) once, and setting

$$\frac{\mathrm{dV}}{\mathrm{d}\xi} = W , \tag{20}$$

we get

$$\frac{\mathrm{d}^2 W}{\mathrm{d}\xi^2} = \alpha W^2 + \beta W + C_1 , \tag{21}$$

with the following abbreviations

$$\alpha = \frac{3}{2}h^{-3} ; \quad \beta = \frac{3\left(\mathrm{v}^2 - gh\right)}{\left(\mathrm{v}h\right)^2} , \tag{22}$$

C_1 is the constant of integration. Taking the next integration of (21) one obtains

$$\frac{1}{2}\left(\frac{\mathrm{d}W}{\mathrm{d}\xi}\right)^2 = \alpha\frac{W^3}{3} + \beta\frac{W^2}{2} + C_1 W + C . \tag{23}$$

When $\mathrm{v}^2 = \mathrm{v}_0^2 = gh$, $\beta = 0$ and above equation reduces to

$$\left(\frac{\mathrm{d}W}{\mathrm{d}\xi}\right)^2 = \frac{2}{3}\alpha W^3 + 2C_1 W + 2C_2 . \tag{24}$$

The solution of this equation can be assumed in the form

$$W = A\theta(\xi) , \tag{25}$$

where $\theta(\xi)$ represents the elliptic function satisfying the differential equation

$$\left(\frac{\mathrm{d}\theta}{\mathrm{d}\xi}\right)^2 = 4\theta^3 - p\theta - q , \tag{26}$$

with the parameters p, q, obeying the condition

$$p^3 - 27q^2 > 0 . \tag{27}$$

Inserting (25) in (24), and equating the coefficients of equal powers of $\theta(\xi)$, one gets

$$\begin{aligned} 4A^2 &= \frac{2\alpha}{3}A^3; \\ -A^2 p &= 2C_1 A; \\ -A^2 q &= 2C_2. \end{aligned} \tag{28}$$

Last equalities yield

$$A = \frac{6}{\alpha}; \quad p = -\frac{\alpha C_1}{3}; \quad q = -\frac{\alpha^2 C_2}{18}. \tag{29}$$

Since parameters p and q satisfy inequality (27), p must be positive imposing that α and C_1 should be of opposite signs, ($C_1 < 0$). The condition (27) implies the restriction

$$4C_1^3 + 9\alpha C_2^2 < 0.$$

The solution of (24) now reads

$$W(\xi) = \frac{6}{\alpha}\theta\left(\xi + C_3;\, p,\, q\right), \tag{30}$$

with new constant of integration C_3. Eventually, the bounded periodic solution is now represented by

$$W\left(\xi\right) = \frac{6}{\alpha}\left[e_3 + \left(e_2 - e_3\right)\mathrm{sn}^2\left(\sqrt{e_1 - e_3}\,\xi + c\right)\right], \tag{31}$$

with arbitrary constant c and parameters e_j (j = 1, 2, 3) being the real roots of the cubic equation

$$4e^3 - pe - q = 0\,; \quad e_1 > e_2 > e_3. \tag{32}$$

Jacobian-sine elliptic function sn follows from relation

$$\theta\left(\xi\right) = e_3 + \left(e_2 - e_3\right)\mathrm{sn}^2\left(\sqrt{e_1 - e_3}\,\xi + c\right). \tag{33}$$

In order to get the solitary wave limit we take the modulus of Jacobian elliptic function defined as

$$m = \frac{e_2 - e_3}{e_1 - e_3}, \tag{34}$$

being equal to unity. In this limit, by using definitions (17) and (20), we get bell-shaped soliton describing in this case giant solitonic water wave (Fig. 2)

$$\eta(x,t) = 4h^3 \left\{ (e_1 - e_3) \sec h^2 \left[\sqrt{e_1 - e_3}\,(x - v_0 t) + c \right] - e_1 \right\}. \tag{35}$$

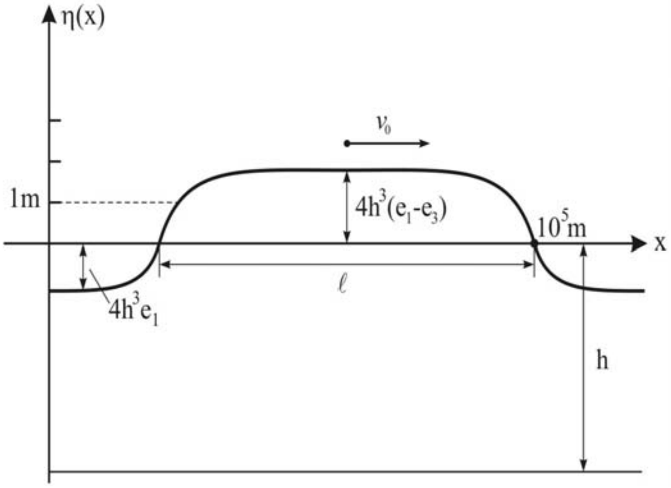

Fig. 2 – The shape of water soliton wave for fixed t with pertaining parameters: speed v_0, length l, depression $4h^3e_1$ and elevation $\eta_0 = 4h^3(e_1 - e_3)$.

Let us just make a simple illustration. If we take the typical ocean depth of the order of $h = 10^3$ m, solitonic speed is of the order of

$$\mathrm{v}_0 = \sqrt{gh} = 10^2\,\frac{\mathrm{m}}{\mathrm{s}} = 360\,\frac{\mathrm{km}}{\mathrm{h}}.$$

The usual length of a soliton created by earth-quake in such depths is of the order of l = 100 km = 10^5 m. It safely satisfies the condition of (5). Consequently, (35) thus gives

$$\sqrt{e_1 - e_3} = 10^{-5}\,\mathrm{m}^{-1}, \quad \text{or} \quad e_1 - e_3 = 10^{-10}\,\mathrm{m}^{-2},$$

yielding, from (32), with appropriate integration constants, to the following real roots

$$e_1 = e_2 = -10^{-10}\,\mathrm{m}^{-2}; \quad e_3 = -2\times 10^{-10}\,\mathrm{m}^{-2}.$$

The corresponding solitonic peak is

$$\eta_0 = 4\times 10^9 \times 5\times 10^{-10}\,\mathrm{m} = 2\mathrm{m}.$$

It brings the realistic, very moderate amplitude which can not be easily identified in the open sea. Numerical solution of this case obtained with the aid of Matlab is shown in Fig. 3.

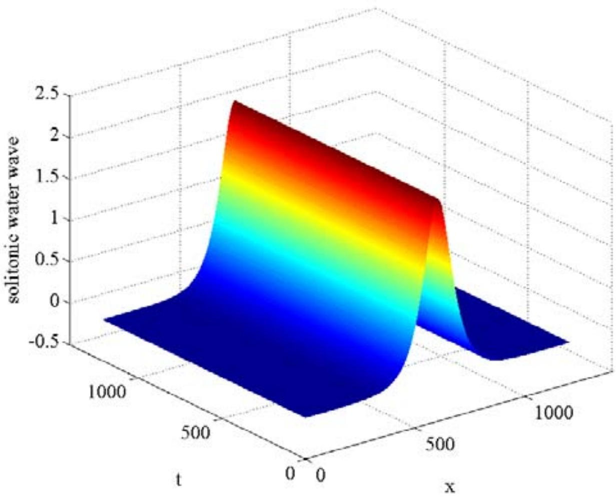

Fig. 3 – Numerical solution of solitonic water wave for ocean depth $h = 10^3$ m, and length $l = 100$ km.

2. NONLINEAR IONIC WAVES ALONG MICROTUBULES

We now examine in more detail a new microscopic biological phenomenon leading to quite analogous equations and pertinent solution as in Section 1. Microtubules (MTs) are cytoskeletal biopolymers made up of GTP-dependent α, β-tubulin protein dimer assemblies [4].

MTs have geometry of long hollow cylinders having outer diameter of 25 nm and inner diameter of 15 nm, with lengths that typically span up to several micrometers (Fig. 4). They consist of 13 parallel protofilaments *in vivo*.

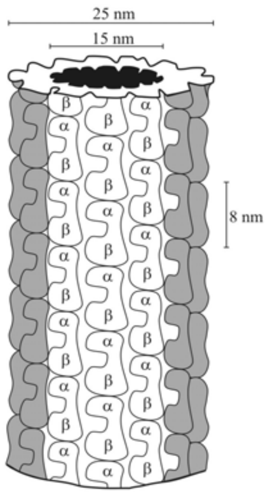

Fig. 4 – A MT hollow cylinder of 13 parallel protofilaments with denoted characteristic dimensions: outer and inner diameters of 25 nm and 15 nm and tubulin dimer length of 8 nm.

Recently it has become apparent that neurons might utilize MT networks in cognitive processing *via* MT associated proteins (MAPs) in neuronal processes such as learning and memory. MTs are also linked to the regulation of a number of ion channels, thus contributing to the electrical activity of excitable cells [5].

Very recently, it was elaborated a new model of MT as the electric nonlinear transmission line [6]. In this reference one could find the details about calculations of capacity, resistivity and inductivity of basic unit of the model. This unit is the elementary ring (ER) consisting of 13 dimers with characteristic dimensions represented in Fig. 5a. Each dimer has two outward protruding rod-like tubulin tails (TTs), Fig. 5a and Fig. 5b. One of them, disposed on β-monomer, is flexible and able to change its length depending on the amount of counter-ions condensed along its negative surface. This circumstance is the essential argument why this model includes the capacity of MT surface which is nonlinear [6].

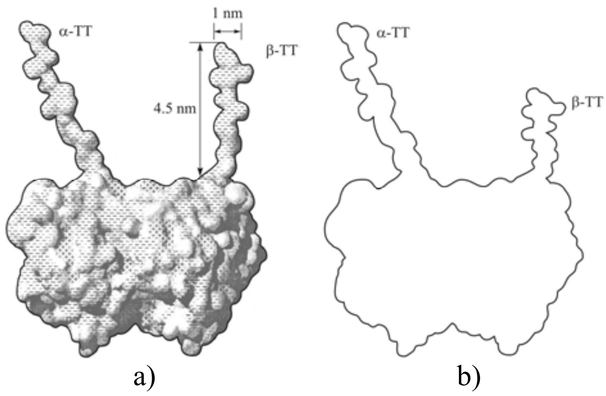

Fig. 5 – a) The landscape of a tubulin dimer with dimensions of TTs the length of 4.5 nm and diameter of 1nm, and surface charge distribution according to Tuszynski et al [7]; b) the shape of TTs, where β-TT is being shrank, thus diminishing its capacity.

The basic idea here is to farther amend the underlying model taking into account the presence and the functions of nano-pores (NPs) embedded in MT wall, as presented in Fig. 6.

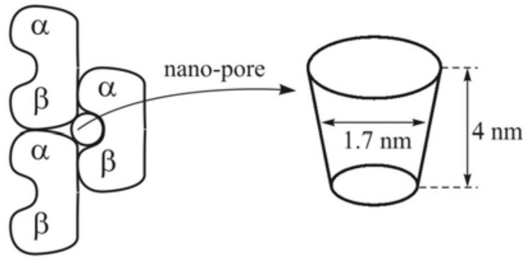

Fig. 6 – The sketch of a NP with approximates shape and dimensions. The conical shape follows from MT geometry.

These NPs act like ionic channels (ionic pumps) according to the investigations performed by the group lead by Eisenberg [8, 9]. This point will be elaborated later in more details. Let us first mention the properties of an ER. MT surface is highly negative due to pertaining amino acids which have lost some protons, according to polyelectrolyte character of MTs. Around MTs surface the ionic cloud (IC) of positive counter-ions is condensed. This IC is separated of bulk cytosol by the shell depleted of any ions (Fig. 7), having the thickness named Bjerrum-length (l_B), estimated to be

$$l_B = \frac{e^2}{4\pi\varepsilon_o \varepsilon k_B \mathrm{T}} = 6.7\times10^{-10}\,\mathrm{m}\,. \tag{36}$$

Here e is the charge of an electron, ε_0 the permittivity of vacuum, $\varepsilon = 80$ the relative permittivity of cytosol, k_B Boltzmann's constant, and $T = 310$ K is the physiological temperature. This depleted shell plays the role of dielectric and confines ionic flow within IC.

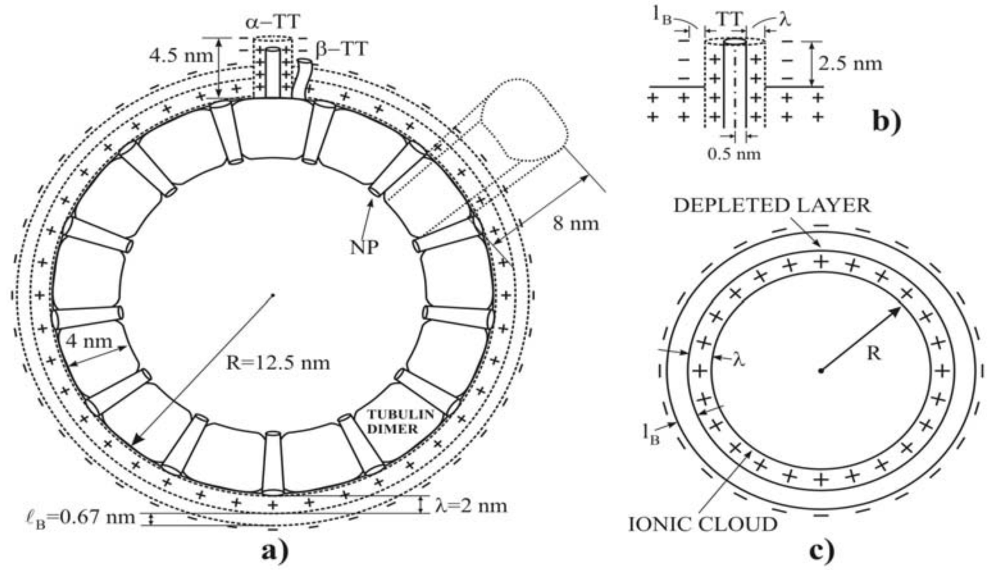

Fig. 7 – The geometry of a MT with ionic cloud and depleted layer clearly depicted, including corresponding dimensions: the thickness of IC: $\lambda = 2$ nm and Bjerrum length, $l_B = 0.67$ nm. The top part of a) shows α and β TTs.

We will here completely omit the calculations of the resistive components of the ER just taking over the values from [6] as follows: the static part of capacity of an ER is estimated to be

$$C_0 = 1.32 \times 10^{-15}\,\text{F}, \tag{37}$$

wile, the inductance is

$$L_0 = 8 \times 10^{-16}\,\text{H}, \tag{38}$$

and longitudinal ohmic resistance amounts

$$R_0 = 10^9\,\Omega. \tag{39}$$

But, since ER's capacitance should change with an increasing concentration of counter-ions, it implies that the charge on this capacitor diminishes with increasing the voltage in a nonlinear way as follows:

$$Q_n = C_0\left(1 - bv_n\right)v_n, \tag{40}$$

where, the parameter b is restricted to obey the inequalities

$$0 < b < 1; \qquad bv_n << 1, \tag{40.a}$$

providing that the change of capacity is being small enough (bv_n<<1), since the change of the area of a β-TT is a few percents of the total outer surface of the corresponding tubulin dimer plus the surface of α-TT. Inasmuch the peak value of v_n *in vivo* is of the order of 0.1 Volt, the condition (40.a) is fulfilled, for example if $b = 0.5$.

We now pay more attention on the role of NPs in the context of negative incremental resistance (conductance). Eisenberg's group [8, 9] examined a single asymmetric NP system whose rectifying properties for ionic current are changed dramatically by addition of a millimolar concentration of calcium ions. The voltage-current function for such NPs exhibits negative incremental resistance for a particular domain of negative voltage across NP, qualitatively represented on Fig. 8 (segment CC').

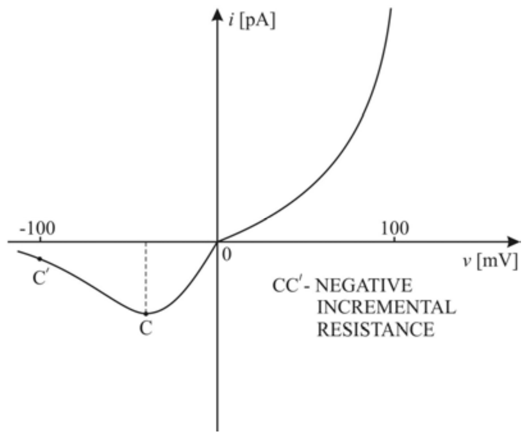

Fig. 8 – The qualitative shape of current-voltage characteristics for NPs in the context of Eisenberg's group's work [8, 9]. The segment CC' shows the negative incremental resistance.

The value of v_c, from Fig. 8, is defined by the structural features of the NP and by the calcium concentration [9]. We are aware that above experiment is far for being adequate for the description of current voltage function for NPs in MT. But some general features could probably hold even for these geometrically and chemically more complex dynamical natural structures. In order take into account dynamic character of conductive properties of NPs in MT we here use the negative conductance of NP to be voltage dependent in a dynamic way as follows:

$$G_n = -G_0\left(1-\gamma\frac{\mathrm{d}v_n}{\mathrm{d}t}\right), \tag{41}$$

with γ being appropriate small parameter providing the inequality

$$\gamma\frac{\mathrm{d}v_n}{\mathrm{d}t} < 1. \tag{41.a}$$

Thus (41) involves an additional nonlinearity of this system.

2.1. The Model of a MT as Nonlinear Transmission Line

We could now consider a long transmission-line (or ladder networks) composed of lumped sections equal to introduced ER's. A typical section scheme is shown in Fig. 9. The length of an ER is Δ = 8 nm is being equal to the length of a tubulin dimmer, Fig 5a. The longitudinal current consists of the series of inductance L_n, which is so small to be safely ignored, and ohmic resistance R_n for IC in an ER as being estimated in Eq. (39). The nonlinear capacity C_n is in parallel with total conductance G_n of all 13 NPs consisted in ER.

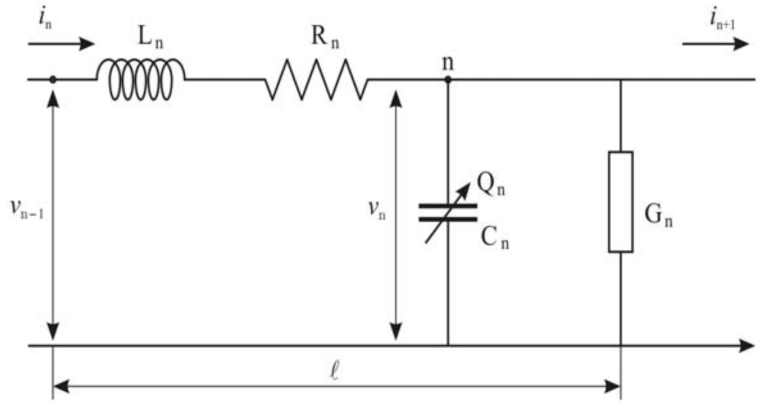

Fig. 9 – An effective circuit diagram for the n-th ER with characteristic elements for Kirchhoff's laws.

Applying Kirchhoff's law to the considered ladder, envisaged as the coupled electrical circuits, we write down

$$i_n - i_{n+1} = \frac{\partial Q_n}{\partial t} + G_n v_n, \tag{42}$$

$$v_{n-1} - v_n = R_n i_n. \tag{43}$$

The important point here is the facts that L_n could be discarded. Inserting (40) and (44) in (42) one gets

$$i_n - i_{n+1} = -G_0 v_n + \gamma G_0 v_n \frac{\partial v_n}{\partial t} + C_0 \frac{\partial v_n}{\partial t} - 2bC_0 v_n \frac{\partial v_n}{\partial t}, \tag{44}$$

$$v_{n-1} - v_n = R_0 i_n \qquad \left(R_n = R_0\right). \tag{45}$$

It is very convenient to establish the characteristic reactive impedance of an ER in a natural way:

$$Z = \frac{1}{C_0 \omega}. \tag{46}$$

It enables us to introduce the new auxiliary function, $u(x, t)$, unifying voltage and current as follows

$$u_n = Z^{1/2} i_n = Z^{-1/2} v_n. \tag{47}$$

Based on the fact that the above functions change gradually from a given ER to its neighbours it is justified to expand u_n in a continuum approximation using a Taylor series in term of a small spatial parameter Δ (the length of an ER):

$$u_{n\pm1} = u \pm \Delta\left(\frac{\partial u}{\partial x}\right) + \frac{\Delta^2}{2!}\left(\frac{\partial^2 u}{\partial x^2}\right) \pm \frac{\Delta^3}{3!}\left(\frac{\partial^3 u}{\partial x^3}\right) + \frac{\Delta^4}{4!}\left(\frac{\partial^4 u}{\partial x^4}\right) \pm \ldots \tag{48}$$

By using (44–48), we now have

$$\begin{aligned}&\frac{\partial u}{\partial x} + \frac{\Delta}{2}\frac{\partial^2 u}{\partial x^2} + \frac{\Delta^2}{6}\frac{\partial^3 u}{\partial x^3} + \frac{\Delta^3}{24}\frac{\partial^4 u}{\partial x^4} + \frac{\Delta^4}{120}\frac{\partial^5 u}{\partial x^5} - \frac{G_0 Z}{\Delta} u + \\ &+ \frac{ZC_0}{\Delta}\frac{\partial u}{\partial t} + \left(\frac{\gamma Z^{3/2} G_0}{\Delta} - \frac{2bZ^{3/2} C_0}{\Delta}\right) u \frac{\partial u}{\partial t} = 0,\end{aligned} \tag{49}$$

$$\frac{\partial u}{\partial x} - \frac{\Delta}{2}\frac{\partial^2 u}{\partial x^2} + \frac{\Delta^2}{6}\frac{\partial^3 u}{\partial x^3} - \frac{\Delta^3}{24}\frac{\partial^4 u}{\partial x^4} + \frac{\Delta^4}{120}\frac{\partial^5 u}{\partial x^5} - \frac{R_0 Z^{-1}}{\Delta} = 0. \tag{50}$$

Combining last two equations and ignoring small terms beyond the order of Δ^3, we get

$$2\frac{\partial u}{\partial x}+\frac{\Delta^2}{3}\frac{\partial^3 u}{\partial x^3}+\frac{1}{\Delta}\left(R_0 Z^{-1}-G_0 Z\right)u+\frac{ZC_0}{\Delta}\frac{\partial u}{\partial t}-\frac{\left(2bC_0-\gamma G_0\right)Z^{3/2}}{\Delta}u\frac{\partial u}{\partial t}=0. \quad (51)$$

The important step in our model is the assumption that the ohmic resistance, R_0, should be balanced by the negative incremental conductance, $-G_0$, thus discarding the third term in (51)

$$\left(R_0 Z^{-1}-G_0 Z\right)=0. \quad (52)$$

Similarly, as in the case of water waves, we should go over to dimensionless variables. Let us first estimate the characteristic scales of length and time. The length of an ER (Δ = 8 nm) is such length. The characteristic time could be the period of charging (discharging) of ER capacitor through the resistance R_0,

$$\tau = R_0 C_0. \quad (53)$$

Taking the numerical values from (37) and (39) we have

$$\tau = 10^9\,\Omega\times 1.32\times 10^{-15}\,\mathrm{F} = 1.32\times 10^{-6}\mathrm{s}. \quad (54)$$

Thus, the characteristic velocity of spreading the ionic wave along the ladder could be estimated as

$$\mathrm{v}_0=\frac{\Delta}{\tau}=\frac{8\times 10^{-9}}{1.32\times 10^{-6}}\frac{\mathrm{m}}{\mathrm{s}}=0.6\frac{\mathrm{cm}}{\mathrm{s}}. \quad (55)$$

It is now convenient to use the progressive traveling-wave form as follows:

$$u(x,t)=u\left(\frac{x}{\Delta}-\mathrm{v}\frac{t}{\Delta}\right)=u\left(\frac{x}{\Delta}-\frac{\mathrm{v}}{\mathrm{v}_0}\mathrm{v}_0\frac{t}{\Delta}\right)=u\left(\frac{x}{\Delta}-s\frac{t}{\tau}\right);\qquad s=\frac{\mathrm{v}}{\mathrm{v}_0}, \quad (56)$$

with dimensionless speed, s. Introducing the new dimensionless space-time variable, ξ

$$\xi=\frac{x}{\Delta}-s\frac{t}{\tau}, \quad (17)$$

one has

$$\frac{\partial u}{\partial x}=\frac{1}{\Delta}\frac{\mathrm{d}u}{\mathrm{d}\xi};\qquad \frac{\partial^3 u}{\partial x^3}=\frac{1}{\Delta^3}\frac{\mathrm{d}^3 u}{\mathrm{d}\xi^3};\qquad \frac{\partial u}{\partial t}=-\frac{s}{\tau}\frac{\mathrm{d}u}{\mathrm{d}\xi}. \quad (58)$$

It enables us to get rid of partial differential equation (51) yielding the ordinary one

$$\frac{\mathrm{d}^3 u}{\mathrm{d}\xi^3}-3\left(\frac{ZC_0 s}{\tau}-2\right)\frac{\mathrm{d}u}{\mathrm{d}\xi}+3\frac{Z^{3/2}s}{\tau}\left(2bC_0-\gamma G_0\right)u\frac{\mathrm{d}u}{\mathrm{d}\xi}=0\ . \quad (59)$$

If we use the definition (47), $u = Z^{1/2}i$, and introduce the dimensionless current

$$W = i / i_0, \tag{60}$$

with i_0 being the peak value, we have

$$u = Z^{1/2} i_0 W = Z^{1/2} i. \tag{61}$$

Replacing (61) into (62) we get

$$\frac{\mathrm{d}^3 W}{\mathrm{d}\xi^3} - 3\left(\frac{ZC_0}{\tau} s - 2\right)\frac{\mathrm{d}W}{\mathrm{d}\xi} + 3\frac{Z^2 i_0 s}{\tau}\left(2bC_0 - \gamma G_0\right) W \frac{\mathrm{d}W}{\mathrm{d}\xi} = 0. \tag{62}$$

Performing first integration yields:

$$\frac{\mathrm{d}^2 W}{\mathrm{d}\xi^2} - 3\left(\frac{ZC_0}{\tau} s - 2\right) W + \frac{1}{2}\left(3\frac{Z^2 i_0 s}{\tau}\left(2bC_0 - \gamma G_0\right)\right) W^2 + C_1 = 0. \tag{63}$$

Comparing (62) with (21) we can use the same abbreviations

$$\alpha = \frac{1}{2}\left(3\frac{Z^2 i_0 s}{\tau}\left(2bC_0 - \gamma G_0\right)\right); \quad \beta = -3\left(\frac{ZC_0}{\tau} s - 2\right). \tag{64}$$

We here also use the conditions $\beta = 0$, leading to the velocity of ionic current defined as

$$s = \frac{2\tau}{ZC_0}. \tag{65}$$

Taking $Z = \frac{1}{C_0 \omega} = \frac{\tau}{C_0 2\pi} = 1.6 \times 10^8\,\Omega$, we get

$$s = 4\pi; \quad \mathrm{v} = 4\pi \mathrm{v}_0 = 7.5\,\frac{\mathrm{cm}}{\mathrm{s}}. \tag{66}$$

This is very interesting intermediate value of biological speed. For example, the speed of ionic diffusion waves in cell is of the order of 10^{-3} cm/s, while the speed of action potential in nerve cell ranges 3×10^3 cm/s. We could finally estimate the term γG_0. From (41) it is possible to average the derivative $\partial v_n / \partial t \approx 0.1/\tau \approx 10^5$. This implies an inequality $\gamma < 10^{-6}$ in order to obey (41.a). Otherwise from (52) we estimate $G_0 = 4\times10^{-8}$ S.

Thus, (63) now reads

$$\frac{\mathrm{d}^2 W}{\mathrm{d}\xi^2} = \alpha W^2 + C_1. \tag{67}$$

Making the next integration of (67) one obtains

$$\left(\frac{\mathrm{d}W}{\mathrm{d}\xi}\right)^2 = \frac{2}{3}\alpha W^3 + 2C_1 W + C_2. \tag{68}$$

This is the same equation as was (24). The remaining formal procedure is already given by set of equations (25-35), yielding

$$\begin{aligned} i(x,t) &= \frac{2\tau}{Z^2\left(2bC_0 - \gamma G_0\right)}\left\{\left(e_1 - e_3\right)\sec h^2\left[\sqrt{e_1 - e_3}\left(x - \mathrm{v}_0 t\right) + c\right] - e_1\right\}; \\ i_0 &= \frac{2\tau}{Z^2\left(2bC_0 - \gamma G_0\right)}. \end{aligned} \tag{69}$$

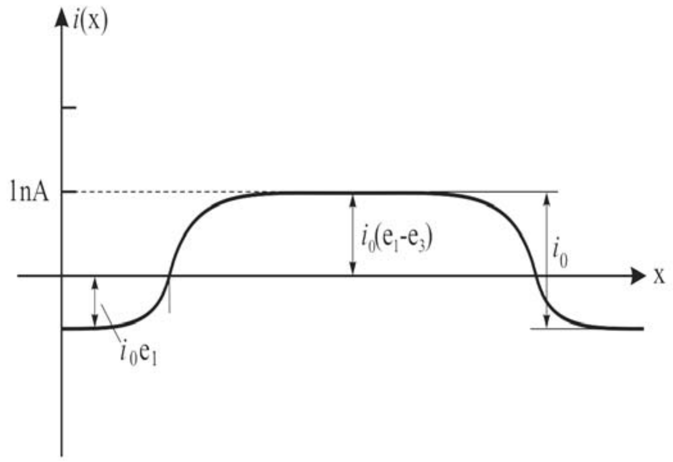

Fig. 10 – The shape of ionic current nano-soliton along a microtubule given for fixed time.

We will now examine the two options of solution of (69). First is the case while the term bC_0 dominates over the NP nonlinearity γG_0, where we have the reductions to the form (Fig. 10)

$$\begin{aligned} i(x,t) &= \frac{\tau}{Z^2 bC_0}\left\{\left(e_1 - e_3\right)\sec h^2\left[\sqrt{e_1 - e_3}\left(x - \mathrm{v}_0 t\right) + c\right] - e_1\right\}, \\ i_0 &= \frac{\tau}{Z^2 bC_0}, \end{aligned} \tag{70}$$

where e_i (i = 1, 2, 3) are the roots of cubic equation:

$$4e^3 - C_1\left(2Zbi_0\right)e + C_2\left(2Zbi_0\right)^2 = 0, \tag{71}$$

and which we will call ionic nano-soliton (INS). Taking $b = 0.1$ V^{-1}, $Z = 1.6\times10^8$ Ω and choosing that i_0 has the order of 10^{-9} A, for appropriate integration constants one gets the following cubic equation

$$e^3 - 3\times10^{-6}e + 2\times10^{-9} = 0, \tag{72}$$

with corresponding roots:

$$e_1 = e_2 = 10^{-3}; \quad e_3 = -2\times10^{-3}. \tag{73}$$

It brings about the width of INS to be of the order of 20 ERs. Numerical solution of this case obtained with the aid of Matlab is shown in Fig. 11.

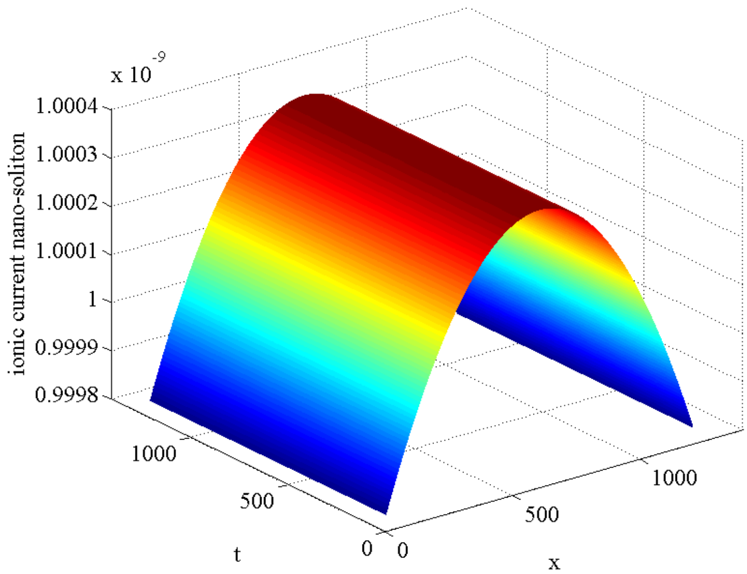

Fig. 11 – Numerical solution of INS along microtubules for $b = 0.1$ V^{-1} and $i_0 = 10^{-9}$ A.

Second option is more realistic while two nonlinearities are competitive. It causes the increase of INS amplitude and brings it more localized. We could comment how the value of frequency ω may influence this competition. If voltage frequency ω changes, the static part of conductivity G_0 also changes through (46, 53)

$$G_0 = \frac{R_0}{Z^2} = R_0 C_0^2 \omega^2. \tag{74}$$

This in order to get γG_0 as being competitive with bC_0, ω should be of the order of 10^3 s^{-1}.

3. CONCLUSIONS AND DISCUSSION

In this paper we have shown how two very different physical phenomena can be described by formally the same mathematical model exhibiting the common features which leads to existence of the permanent profile bell-shaped soliton solutions.

It results from equilibrium between two effects, the nonlinearity that tends to localize the wave, while dispersion spreads it out. The origins of respective nonlinearities are quite different. In the case of water waves the nonlinearity originates from kinetic energy, contained in Euler's equation (2). In the other hand, the potential energy of ionic wave within INS along MTs captures nonlinearity from biophysical properties enabling the change of ER capacity and NPs conductivity according to equations (40, 41).

We here paid more attention to the INSs along MTs due to the importance of this subtle phenomenon in better understanding of basic neuronal functions, including learning and memory processes.

Our present model offers the satisfactory results regarding orders of magnitude of ionic current, speed of pertaining INSs in the context of still scarce available experimental evidences.

We especially mention an interesting experimental assay performed by the group led by Tuszynski [11]. They have calculated that electrical amplification of ionic currents by MTs is in some sense equivalent to their ability to act as biomolecular living transistors. In that respect the current of ions pumped by NPs in negative resistance regime, equation (52), is expected to play the control role, as well as the base current does play in silicon bipolar transistor.

Acknowledgments. This research was supported by funds of Serbian Ministry of Science, Grants: III 43008, III 45003 and 171009, and Serbian Academy of Sciences and Arts.

REFERENCES

1. L. Debnath, *Nonlinear Water Waves*, Academic Press, New York, 1994.
2. J. Falnes, *Ocean Waves and Oscillating Systems*, Cambridge University Press, Cambridge, 2002.
3. T. Dauxois and M. Peyrard, *Physics of Solitons*, Cambridge University Press, Cambridge, 2006.
4. P. Dustin, *Microtubules*, 2nd Edition, Springer, Berlin, 1984.
5. B. D. Johnson and L. Byerly, Am. J. Physiology, **266**, L681 (1994).
6. M. V. Satarić, D. I. Ilić, N. Ralević and J. A. Tuszynski, Eur. Biophys. J., **38**, 637 (2009).
7. J. A. Tusyznski, J. A. Brown, E. Crowford, E. J. Carpenter, M. L. A. Nip, J. M. Dixon and M. V. Satarić, Math. Comput. Model, **41**, 1055 (2005).
8. Z. S. Siwy, M. R. Powell, E. Kalman, R. D. Astumian. and R. S. Eisenberg, Nano. Lett., **6**, 473 (2006).
9. Z. S. Siwy, M. R. Powell, A. Petrov, E. Kalman, C. Trantmann and R. S. Eisenberg Nano. Lett., **6**, 1729 (2006).
10. E. C. Lin and H. F. Cantiello, Biophys. J., **65**, 1371 (1993).
11. A. Priel, A. J. Ramos, J. A. Tuszynski and H. F. Contiello, Biophys. J., **40**, 1 (2006).